PHYSICAL REVIEW B **91**, 180502(R) (2015)

Pressure-induced decomposition of solid hydrogen sulfide

Defang Duan, Xiaoli Huang, Fubo Tian, Da Li, Hongyu Yu, Yunxian Liu, Yanbin Ma, Bingbing Liu, and Tian Cui*
State Key Laboratory of Superhard Materials, College of Physics, Jilin University, Changchun 130012, People's Republic of China
(Received 13 January 2015; revised manuscript received 30 March 2015; published 12 May 2015)

Solid hydrogen sulfide is a typical molecular crystal, but its stability under pressure remains controversial. In particular, the recent experimental discovery of high-pressure superconductivity at 190 K in an H_2S sample (arXiv:1412.0460) inspired efforts to revalidate this controversial issue, the pressure at which H_2S decomposes and the resultant decomposition products urgent need to be evaluated. In this paper we performed an extensive structural study on different stoichiometries of H_nS with $n > 1$ under high pressure using *ab initio* calculations. Our results show that H_2S is stable below 43 GPa and at elevated pressure it decomposes into H_3S and sulfur. H_3S is stable at least up to 300 GPa, while other H-rich compounds, including H_4S, H_5S, and H_6S, are unstable in the pressure range of this study.

DOI: 10.1103/PhysRevB.91.180502 PACS number(s): 74.62.Fj, 61.50.Ks, 74.70.Ad, 82.33.Pt

I. INTRODUCTION

Solid hydrogen sulfide is a typical molecular crystal that has been studied extensively at high pressure [1–15]. To date, however, the exact structures and molecular dissociation of H_2S at high pressure remains controversial. Experimentally, hydrogen sulfide transforms into phase IV with monoclinic *Pc* [8] or tetragonal $I4_1/acd$ [9] at room temperature. Upon compression, further transformation is complicated by dissociation of H_2S molecules. It is reported that H_2S molecules dissociate into H and S atoms above 46 GPa at room temperature by infrared-absorption spectral measurement [6]. In addition, x-ray powder diffraction revealed that solid H_2S decomposes into element S above 27 GPa at room temperature and higher pressure of approximately 43 GPa at 150 K [13]. The Raman and IR spectra of D_2S have found that it partially decomposes into sulfur and several kinds of S-D or S-S bonds at pressures above 27 GPa and room temperature [12]. Metallization of H_2S occurs near 96 GPa [6], which can be attributed to elemental sulfur; this element is known to become metallic above 95 GPa [16].

Theoretically, Rousseau *et al.* examined the structure and stability of H_2S at room temperature through *ab initio* molecular dynamics (MD) simulations. They suggested that phase IV exhibits partial rotational disorder with $P4_2/ncm$ [10] and that H_2S molecules lose their identity in phase V by forming H_3S^+ and HS^- ionic species [11]. Another *ab initio* MD simulation predicted an *Ibca* structure at 15 GPa and 100 K [14]. When temperature is increased to 350 K, the *Ibca* structure transforms into a proton disorder structure, which is important to the decomposition of H_2S. Recent theoretical studies [15] have predicted several high phases of H_2S and suggested that H_2S is stable with respect to elemental decomposition into S and H_2 up to 200 GPa.

Recently we have extensively explored the high-pressure structures and superconductivity of an experimentally synthesized $(H_2S)_2H_2$ compound [17] through *ab initio* calculations [18]. In this work we found four high-pressure phases and predicted the T_c of the $Im\text{-}3m$ phase to reach 191–204 K at 200 GPa. Excitingly, superconductivity in an H_2S sample with high $T_c = 190$ K above 150 GPa has been observed recently [19]. In this experimental research, they found the precipitation of S. So they speculated the superconductivity associates with the formation of H-enriched H_nS ($n > 2$) hydrides according to our earlier theoretical studies [18].

The previous theoretical studies on H_2S only demonstrated that they are stable with respect to H_2 and S at high pressure [11,15]. However, the stability of H_2S against decomposition into other stoichiometric compounds, e.g., H_3S, H_4S, H_5S, or H_6S, which is very important for understanding the superconducting phase in recent experiments, has not been investigated to this day. Therefore, in the present study we aim to elucidate the high-pressure stability of different stoichiometric H_nS ($n > 1$) using *ab initio* calculations. We also investigate whether or not H_2S can decompose and determine decomposition products. Results show that H_2S are only stable below 43 GPa and above that pressure they decomposes into H_3S and elemental sulfur.

II. COMPUTATIONAL DETAILS

Stable compounds and structures with different stoichiometric H_nS ($n > 1$) were explored by merging the evolutionary algorithm and *ab initio* total-energy calculations, as implemented in the USPEX code (Universal Structure Predictor: Evolutionary Xtallography) [20–22]. This method employed here are designed requiring only chemical compositions for a given compound to search for stable or metastable structures at given pressure conditions. The details of this search algorithm and its applications have been described elsewhere [23,24]. Underlying structural relaxations are performed using density functional theory as implemented in the Vienna *ab initio* simulation package of the VASP code [25]. The generalized gradient approximation of Perdew-Burke-Ernzerhof [26] is adopted to describe the exchange-correlation potential, and projector augmented wave (PAW) potentials [27] are used to describe the ionic potentials. Owing to the reduced bond lengths under pressure, the "hard" PAW potential are adopted with core radii of 0.8 au for H ($1s^2$) and 1.5 au for S ($3s^2 3p^4$). For the initial searching structures, Brillouin zone sampling using a grid spacing of $2\pi \times 0.05$ Å^{-1} and a plane-wave basis set cutoff of 500 eV are found to be sufficient. However, we recalculate the enthalpy curves with higher accuracy using the

*cuitian@jlu.edu.cn

energy cutoff of 800 eV and k mesh of $2\pi \times 0.03$ Å^{-1} within the Monkhorst-Pack scheme to ensure that the total energies are well converged to better than 1 meV/atom.

III. RESULTS AND DISCUSSIONS

The structural predictions are performed by considering simulation sizes ranging from 1 to 4, 6, and 8 formula units per cell (fu/cell) for H_2S and H_3S in the pressure range from 20 to 300 GPa. For the case of H_4S, H_5S, and H_6S, the structure predictions are performed within 2 and 4 fu at pressures of 50, 100, 200, and 300 GPa. The stability of H_nS ($n > 1$) can be quantified by constructing the thermodynamic convex hull at the given pressure and 0 K, which is defined as the formation enthalpy per atom of the most stable phases at each stoichiometry:

$$h_f(\mathrm{H}_n\mathrm{S}) = [h(\mathrm{H}_n\mathrm{S}) - h(\mathrm{S}) - nh(\mathrm{H}_2)/2]/(n+1),$$

where h_f is the enthalpy of formation per atom and h is the calculated enthalpy per stoichiometric unit for each compound. The enthalpies h for H_nS are obtained for the most stable structures as searched by the USPEX method at the desired pressures. The known structures of $P6_3/m$, $C2/c$, and $Cmca$ [28] for H_2, $I4_1/acd$ [29] and β-Po [30] for S are adopted in their corresponding stable pressure. Any structure with its enthalpy on the convex hull is considered to be thermodynamically stable and experimentally synthesizable [31]. The convex hulls at selected pressure of H_nS are depicted in Fig. 1.

If a tieline is drawn to connect h_f (A) and h_f (B), and h_f (C) falls beneath it, compounds A and B will react to form compound C, provided that the kinetic barrier is not too high. If another compound D with h_f (D) falls above the tieline that connects h_f (A) and h_f (B), compound D is expected to decompose into compounds A and B. The solid line in Fig. 1 traces the estimated convex hulls of stoichiometries of H_nS ($n > 1$) at 20, 40, 50, 100, 200, and 300 GPa. At 20 GPa [Fig. 1(a)], the enthalpies of formation for H_2S and H_3S fall on the convex hull, which indicates that both compounds are thermodynamically stable at this pressure. In addition, H_2S has the most negative enthalpy of formation, which is consistent with the fact that H_2S exists at a low pressure range. From the convex hulls, H_3S can be synthesized using S and H_2 or H_2S and H_2 as precursors; in fact, the latter scenario, i.e., $2H_2S + H_2 \rightarrow 2H_3S$, has been confirmed by Strobel *et al.* [17]. The group reported that mixtures of H_2S and H_2 loaded into diamond anvil cells and compressed up to 3.5 GPa can form a compound $(H_2S)_2H_2$ (H_3S with a H:S stoichiometric ratio of 3:1).

As pressure increased, H_3S became the most stable stoichiometry, and H_2S began to deviate from the tieline at 50 GPa [Fig. 1(c)]. This phenomenon clearly suggests that H_2S is unstable and will decompose into H_3S and sulfur via the reaction $3H_2S \rightarrow 2H_3S + S$. It is shown that H_3S remains as the most stable stoichiometry up to 300 GPa, which is the highest pressure examined in the current study. The calculations further showed that the H_4S, H_5S, and H_6S stoichiometries are unstable and decomposes into H_3S and H_2 in our studied pressure range via the reactions $2H_4S \rightarrow 2H_3S + H_2$, $H_5S \rightarrow H_3S + H_2$, and $2H_6S \rightarrow 2H_3S + 3H_2$. Therefore, the hypothetical decompositions of $2H_2S \rightarrow H_4S + S$, $5H_2S \rightarrow 2H_5S + 3S$, and $3H_2S \rightarrow H_6S + 2S$ are energetically unfavorable. Based on the recent experimental [17,19] and present theoretical studies, H_3S compound can be obtained through two approaches, that is, by compressing pure H_2S sample or mixtures of H_2S and H_2.

Furthermore, the enthalpies of the decomposition (H_3S + S) relative to that of the H_2S as a function of pressure have been

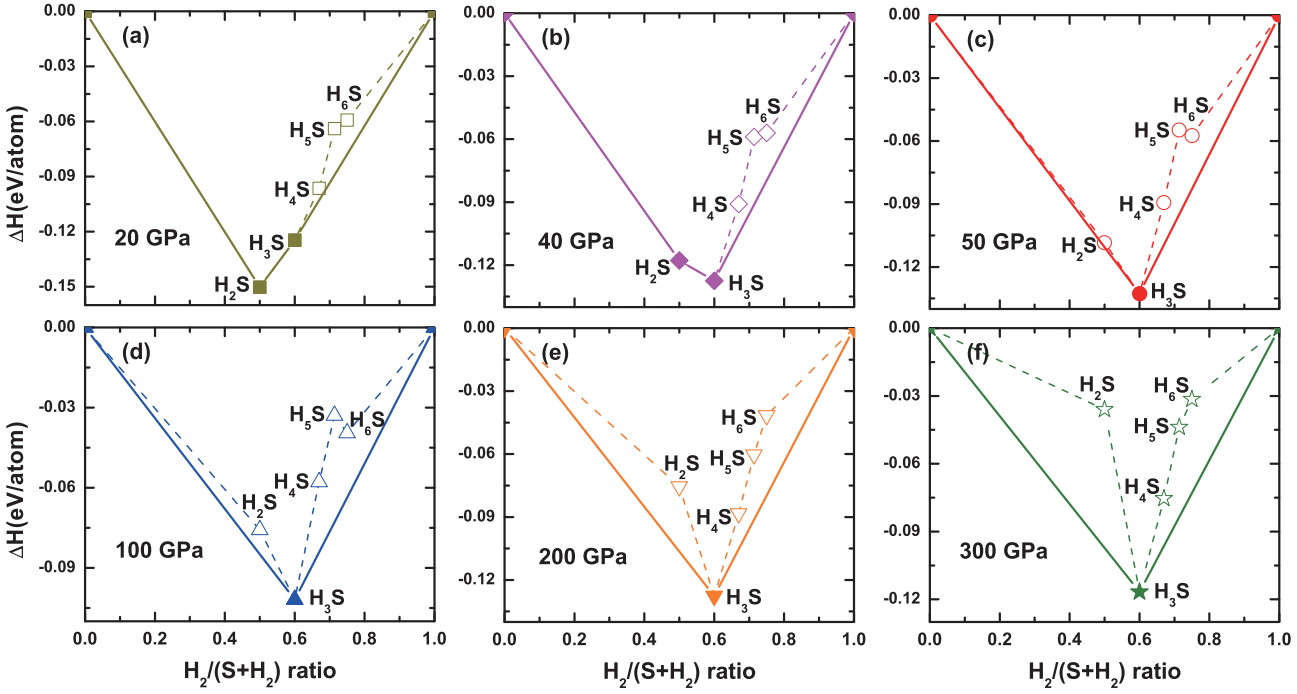

FIG. 1. (Color online) Predicted formation enthalpies of H_nS with respect to decomposition into S and H_2 under pressure. Dashed lines connect data points, and solid lines denote the convex hull.

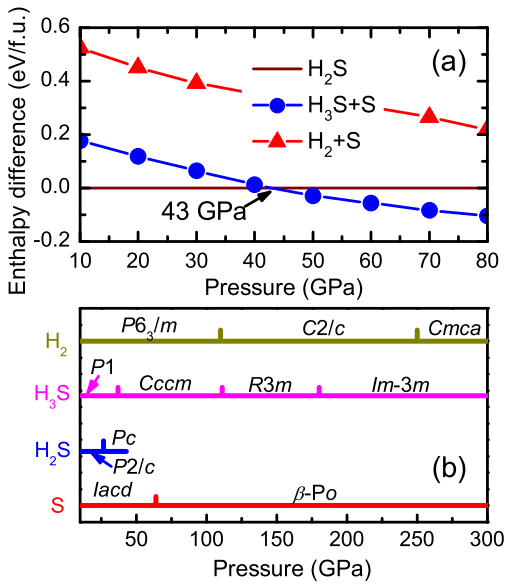

FIG. 2. (Color online) (a) Enthalpies of decomposition of H_2S into H_3S + S and H_2 + S as a function of pressure. (b) Schematic representation of phase diagram for stable H_nS compounds including H_2 [28] and S [29,30] at 0 K as a function of pressure.

plotted in Fig. 2(a) to confirm the decomposition pressure of H_2S. It is more clearly seen that H_2S decomposes into H_3S and S above 43 GPa. In addition, the enthalpies of various phases for H_2S and H_3S as a function of pressure are predicted in Fig. S1 of the Supplemental Material [32]. The stable pressure ranges of various phases for stable H_nS compounds (H_2S and H_3S) are depicted in Fig. 2(b). It is shown that H_2S is stable below 43 GPa and the $P2/c$ phase transforms to Pc phase at 27 GPa. It is noted that H_3S is stable up to 300 GPa, and the phase transition sequence with increasing pressure is from triclinic $P1$ to orthorhombic $Cccm$ at 37 GPa, to trigonal $R3m$ at 111 GPa, then to cubic Im-3m at 180 GPa. In addition, we also showed the stable pressure ranges for H_2 and S in Fig. 2(b).

The stable structures calculated for each stoichiometry are shown in Fig. 3. H_2S is stable in $P2/c$ and Pc structures, which is in agreement with recent theoretical results by Li *et al.* [15], as shown in Figs. 3(a) and 3(b). At higher pressures, H_2S decomposes into H_3S and S at 43 GPa, consistent with experimental observations of H_2S molecular dissociation near 43 GPa at 150 K [13]. Moreover, in the recent experiment [19], an abrupt change in the Raman spectra and H_2S sample was observed at ∼50 GPa, which indicates a structural transition at this pressure.

The high-pressure structures, metallization, and superconductivity of the H_3S stoichiometry have been elucidated in our previous study [18]. At 20 GPa, H_3S adopts a $P1$ structure, which consists of an ordered H-bonded H_2S network [Fig. 3(c)]. Above 37 GPa, the $Cccm$ structure is energetically favored with partial hydrogen bond symmetrization [Fig. 3(d)]. On further compression, two intriguing metallic structures with $R3m$ and Im-3m symmetries [Figs. 3(e) and 3(f)] are reconstructed above 111 and 180 GPa, respectively. The Im-3m structure is characterized by S atoms located at a simple body-centered cubic lattice and H atoms located symmetrically between S atoms. Application of the Allen-Dynes-modified McMillan equation for the Im-3m phase yields high T_c values

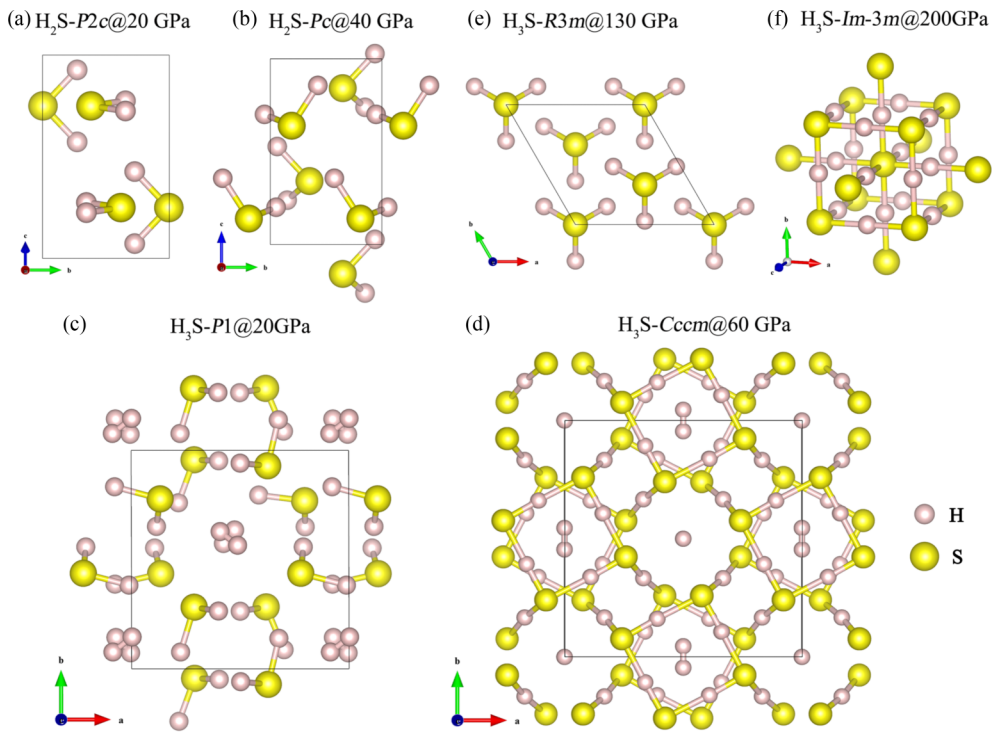

FIG. 3. (Color online) Stable structures of H_2S and H_3S stoichiometries. (a) H_2S at 20 GPa in a $P2c$ structure. (b) H_2S at 40 GPa in a Pc structure. (c) H_3S at 20 GPa in a $P1$ structure. (d) H_3S at 60 GPa in a $Cccm$ structure. (e) H_3S at 130 GPa in a R-3m structure. (f) H_3S at 200 GPa in a Im-3m structure. Large yellow spheres represent S atoms and small pink spheres denote H atoms, respectively.

of 191 to 204 K at 200 GPa, and T_c decreases with increasing pressure.

Although the H_4S, H_5S, and H_6S stoichiometries are only metastable, the evolution of their crystal structures compared with H_3S is worthy of exploration. Selected structures of H_4S, H_5S, and H_6S at 200 and 300 GPa are shown in Fig. S2 in the Supplemental Material [32]. H_4S forms an orthorhombic structure with *Fmmm* symmetry (16 fu/cell) at 200 GPa. In this structure, the coordination number of the S atom is six, which is the same as that in the Im-3m phase of H_3S. In addition, H_2 molecular units are found between H_3S Im-3m blocks. At 200 GPa, H_5S and H_6S form an orthorhombic structure with *Fmmm* symmetry (8 fu/cell) and *Cmma* symmetry (4 fu/cell), respectively. H_4S, H_5S, and H_6S exhibit a common feature at 200 GPa, that is, they all consist of H_3S Im-3m blocks embedded with H_2 molecular units that form a sandwich-type structure. This characteristic suggests the possibility of decomposition into a mixture H_3S and H_2. By contrast, H_2 molecular units disappear in the H_6S-*Pbcn* structure, which is characterized by six H-S bonds in the H_6S molecular unit at 300 GPa [Fig. S2(d)]. This phenomenon suggests that H_6S may become stable at higher pressures.

Figure 1(d) shows that H_2S clearly deviates from the tieline at 200 GPa, and H_3S has the most negative enthalpy of formation. From the combination of the recent experimental observation T_c of the H_2S sample [19] and previously theoretical studies on superconductivity of $(H_2S)_2H_2$ [18], we obtained a significant conclusion that the high T_c of 190 K in the recent experiment at 200 GPa comes from the Im-3m phase of H_3S. Our present work is important for the further relevance of any calculations to the experiments in Ref. [19]. For H_2S in Ref. [15], they only discuss that H_2S are stable relative to S + H_2, while the enthalpies of H_2S relative to H_3S + S is not involved. So they cannot obtain the important physical information that H_2S decomposes into H_3S and S at high pressure. In addition, the high T_c of 80 K in the *Cmca* phase at 160 GPa mainly arises from the sharply elevated N_F. Moreover, the S and H vibrations contribution to the electron phonon coupling (EPC) λ is approximately equal due to forming the S-S bond. For the *Im*-3*m* phase of H_3S at 200 GPa, the high T_c (191–204 K) mainly attributed to the strong EPC λ of 2.19. It is shown that the S vibrations and H vibrational mode contribute 18.4% and 82.6% to the total λ, respectively. Therefore, the H vibrations play a significant role because of one more H atom formed H-S bond.

IV. CONCLUSIONS

In summary, we have explored the phase stabilities and structures of different stoichiometries of H_nS ($n > 1$) at high pressure through *ab initio* calculations. The results demonstrate that H_2S decomposes into H_3S and S above 43 GPa and that H_3S is stable up to 300 GPa. By contrast, other H-rich compounds, namely, H_4S, H_5S, and H_6S, are unstable in the pressure range examined. Therefore, the H_2S sample exhibiting superconductivity at 190 K in Ref. [19] comes from the Im-3m phase of H_3S. Our findings provide the key information for understanding the superconducting phase and renew the knowledge of general understanding that hydrides decompose to elementary species under high pressure. It is greatly helpful for studying the other hydrides at high pressure, e.g., HBr, SiH_4, and alkali metal hydride. Further experimental studies of H_2S and pure H_3S at high pressure are still greatly demanded.

Note added in proof. Recently we became aware of several articles [33–35] that confirmed our results using different structural search techniques.

ACKNOWLEDGMENTS

This work was supported by the National Basic Research Program of China (No. 2011CB808200), Program for Changjiang Scholars and Innovative Research Team in University (No. IRT1132), National Natural Science Foundation of China (No. 51032001, No. 11204100, No. 11074090, No. 10979001, No. 51025206, and No. 11104102), National Found for Fostering Talents of basic Science (No. J1103202), and China Postdoctoral Science Foundation (2012M511326 and 2013T60314). Parts of the calculations were performed in the High Performance Computing Center (HPCC) of Jilin University.

[1] H. Shimizu, Y. Nakamichi, and S. Sasaki, J. Chem. Phys. **95**, 2036 (1991).
[2] H. Shimizu, H. Murashima, and S. Sasaki, J. Chem. Phys. **97**, 7137 (1992).
[3] S. Endo, N. Ichimiya, K. Koto, S. Sasaki, and H. Shimizu, Phys. Rev. B **50**, 5865 (1994).
[4] H. Shimizu, H. Yamaguchi, S. Sasaki, A. Honda, S. Endo, and M. Kobayashi, Phys. Rev. B **51**, 9391 (1995).
[5] S. Endo, A. Honda, S. Sasaki, H. Shimizu, O. Shimomura, and T. Kikegawa, Phys. Rev. B **54**, R717 (1996).
[6] M. Sakashita, H. Yamawaki, H. Fujihisa, K. Aoki, S. Sasaki, and H. Shimizu, Phys. Rev. Lett. **79**, 1082 (1997).
[7] H. Shimizu, T. Ushida, S. Sasaki, M. Sakashita, H. Yamawaki, and K. Aoki, Phys. Rev. B **55**, 5538 (1997).
[8] S. Endo, A. Honda, K. Koto, O. Shimomura, T. Kikegawa, and N. Hamaya, Phys. Rev. B **57**, 5699 (1998).
[9] H. Fujihisa, H. Yamawaki, M. Sakashita, K. Aoki, S. Sasaki, and H. Shimizu, Phys. Rev. B **57**, 2651 (1998).
[10] R. Rousseau, M. Boero, M. Bernasconi, M. Parrinello, and K. Terakura, Phys. Rev. Lett. **83**, 2218 (1999).
[11] R. Rousseau, M. Boero, M. Bernasconi, M. Parrinello, and K. Terakura, Phys. Rev. Lett. **85**, 1254 (2000).
[12] M. Sakashita, H. Fujihisa, H. Yamawaki, and K. Aoki, J. Phys. Chem. A **104**, 8838 (2000).
[13] H. Fujihisa, H. Yamawaki, M. Sakashita, A. Nakayama, T. Yamada, and K. Aoki, Phys. Rev. B **69**, 214102 (2004).
[14] L. Wang, F. Tian, W. Feng, C. Chen, Z. He, Y. Ma, T. Cui, B. Liu, and G. Zou, J. Chem. Phys. **132**, 164506 (2010).

[15] Y. Li, J. Hao, H. Liu, Y. Li, and Y. Ma, J. Chem. Phys. **140**, 174712 (2014).
[16] S. Kometani, M. I. Eremets, K. Shimizu, M. Kobayashi, and K. Amaya, J. Phys. Soc. Jpn. **66**, 2564 (1997).
[17] T. A. Strobel, P. Ganesh, M. Somayazulu, P. R. C. Kent, and R. J. Hemley, Phys. Rev. Lett. **107**, 255503 (2011).
[18] D. Duan, Y. Liu, F. Tian, D. Li, X. Huang, Z. Zhao, H. Yu, B. Liu, W. Tian, and T. Cui, Sci. Rep. **4**, 6968 (2014).
[19] A. P. Drozdov, M. I. Eremets, and I. A. Troyan, arXiv:1412.0460.
[20] A. R. Oganov and C. W. Glass, J. Chem. Phys. **124**, 244704 (2006).
[21] A. R. Oganov, A. O. Lyakhov, and M. Valle, Acc. Chem. Res. **44**, 227 (2011).
[22] A. O. Lyakhov, A. R. Oganov, H. T. Stokes, and Q. Zhu, Comput. Phys. Commun. **184**, 1172 (2013).
[23] A. R. Oganov, J. Chen, C. Gatti, Y. Ma, Y. Ma, C. W. Glass, Z. Liu, T. Yu, O. O. Kurakevych, and V. L. Solozhenko, Nature (London) **457**, 863 (2009).
[24] Y. Ma, M. Eremets, A. R. Oganov, Y. Xie, I. Trojan, S. Medvedev, A. O. Lyakhov, M. Valle, and V. Prakapenka, Nature (London) **458**, 182 (2009).
[25] G. Kresse and J. Furthmüller, Phys. Rev. B **54**, 11169 (1996).
[26] J. P. Perdew, K. Burke, and M. Ernzerhof, Phys. Rev. Lett. **77**, 3865 (1996).
[27] G. Kresse and D. Joubert, Phys. Rev. B **59**, 1758 (1999).
[28] C. J. Pickard and R. J. Needs, Nat. Phys. **3**, 473 (2007).
[29] O. Degtyareva, E. Gregoryanz, M. Somayazulu, P. Dera, H.-k. Mao, and R. J. Hemley, Nat. Mater. **4**, 152 (2005).
[30] H. Luo, R. G. Greene, and A. L. Ruoff, Phys. Rev. Lett. **71**, 2943 (1993).
[31] J. Feng, R. G. Hennig, N. W. Ashcroft, and R. Hoffmann, Nature (London) **451**, 445 (2008).
[32] See Supplemental Material at http://link.aps.org/supplemental/10.1103/PhysRevB.91.180502 for brief description.
[33] N. Bernstein, C. S. Hellberg, M. D. Johannes, I. I. Mazin, and M. J. Mehl, Phys. Rev. B **91**, 060511 (2015).
[34] J. A. Flores-Livas, A. Sanna, and E. K. U. Gross, arXiv:1501.06336.
[35] I. Errea, M. Calandra, C. J. Pickard, J. Nelson, R. J. Needs, Y. Li, H. Liu, Y. Zhang, Y. Ma, and F. Mauri, Phys. Rev. Lett. **114**, 157004 (2015).